Cell

A Class of Membrane Proteins Shaping the Tubular Endoplasmic Reticulum

Gia K. Voeltz,[1] William A. Prinz,[2] Yoko Shibata,[1] Julia M. Rist,[1] and Tom A. Rapoport[1,*]
[1] Howard Hughes Medical Institute and Department of Cell Biology, Harvard Medical School, 240 Longwood Avenue, Boston, MA 02115, USA
[2] Laboratory of Cell Biochemistry and Biology, NIDDK, National Institutes of Health, Bethesda, MD 20892, USA
*Contact: tom_rapoport@hms.harvard.edu
DOI 10.1016/j.cell.2005.11.047

SUMMARY

How is the characteristic shape of a membrane bound organelle achieved? We have used an in vitro system to address the mechanism by which the tubular network of the endoplasmic reticulum (ER) is generated and maintained. Based on the inhibitory effect of sulfhydryl reagents and antibodies, network formation in vitro requires the integral membrane protein Rtn4a/NogoA, a member of the ubiquitous reticulon family. Both in yeast and mammalian cells, the reticulons are largely restricted to the tubular ER and are excluded from the continuous sheets of the nuclear envelope and peripheral ER. Upon overexpression, the reticulons form tubular membrane structures. The reticulons interact with DP1/Yop1p, a conserved integral membrane protein that also localizes to the tubular ER. These proteins share an unusual hairpin topology in the membrane. The simultaneous absence of the reticulons and Yop1p in *S. cerevisiae* results in disrupted tubular ER. We propose that these "morphogenic" proteins partition into and stabilize highly curved ER membrane tubules.

INTRODUCTION

Many organelles have characteristic shapes that often deviate significantly from spheres, likely the energetically most stable form of a membrane bound object. An example is the endoplasmic reticulum (ER), which consists of two major, differently shaped domains: the nuclear envelope (NE) and the peripheral ER (Baumann and Walz, 2001; Du et al., 2004; Voeltz et al., 2002). The NE consists of two continuous sheets of membranes, the inner and outer nuclear membrane, connected to one another at nuclear pores. The approximately spherical shape of the NE is stabilized by interactions between inner nuclear membrane proteins and the underlying chromatin and—in higher eukaryotes—the nuclear lamina (Holmer and Worman, 2001). The peripheral ER consists of a network of membrane tubules connected by three-way junctions. It also contains membrane sheets (cisternae), particularly close to the nucleus, which are prominent in secretory cells (Baumann and Walz, 2001). In mammalian cells, the peripheral ER extends from the NE throughout the entire cell, while in *S. cerevisiae*, it is located beneath the plasma membrane, linked by a few tubules to the NE (Prinz et al., 2000). The entire ER is a continuous membrane system enclosing a single luminal space.

The mechanism by which the tubular ER is generated and maintained is unclear. One idea is that membrane tubules are generated by being pulled out by molecular motors as they move along microtubule or actin filaments or by the tips of filaments as these grow by polymerization (for review, see Du et al., 2004). Although the cytoskeleton is indeed required for dynamic movements of the ER network, the alignment of membrane tubules with microtubules in mammalian cells and with actin in plants and yeast is not perfect (Prinz et al., 2000; Staehelin, 1997; Terasaki et al., 1986), and the network only retracts slowly upon depolymerization of microtubules (Terasaki et al., 1986). Thus, the cytoskeleton does not seem to be essential to maintain ER tubules. In addition, when ER networks are formed in vitro from small vesicles, an intact microtubule or actin network is not required (Dreier and Rapoport, 2000). Other models of ER network formation and maintenance postulate the existence of abundant scaffolding proteins inside or outside of the ER or the regulation of internal ER volume by ion pumps and water flow restriction (Voeltz et al., 2002). However, scaffolds are not obvious in electron microscopy pictures and would be difficult to reconcile with the dynamic nature of the ER tubules, and the ER membrane is permeable to small molecules (Le Gall et al., 2004). Perhaps the most plausible models for tubule formation and maintenance are based on mechanisms that generate or stabilize high curvature in membranes. For example, the high curvature in cross-sections of the tubules could be generated if the two leaflets of a membrane had different lipid compositions (for review, see Farsad and De Camilli, 2003; Sprong et al., 2001). Proteins would be required to keep the lipid imbalance or to create curvature on their own.

Here we have used an in vitro system as the starting point to identify membrane proteins involved in ER network formation. Based on localization, overexpression, and deletion experiments, we reach the conclusion that the reticulons and the interacting protein DP1/Yop1p are the major components shaping the tubular ER.

RESULTS

In Vitro ER Formation

To identify components required for tubular ER formation, we used a previously established in vitro system (Dreier and Rapoport, 2000). The starting material were small (50–100 nm) salt-washed membrane vesicles from *Xenopus laevis* eggs that are devoid of cytosolic proteins and depleted of peripheral membrane proteins (see Figure S1 in the Supplemental Data available with this article online). When these vesicles were incubated at 25ºC in the presence of GTP, they fused to form an elaborate network (Figure 1A, lower versus upper left panels) that could also be stained with antibodies to an ER marker but not with antibodies to other organelles (Dreier and Rapoport, 2000). Efficient network formation occurred at 200 mM salt in the absence of cytosol; at low salt (50 mM), larger vesicles appeared instead (Figure 1A, lower right panel). In the absence of GTP (Figure 1A, upper right panel) or in the presence of GTPγS (Dreier and Rapoport, 2000), neither networks nor large vesicles were formed, suggesting that GTP hydrolysis is required for fusion during tubule and large-vesicle formation.

Because only a small portion of the sample is analyzed in the visual assay, we developed a quantitative and more objective assay for network formation, similar to one used to measure vacuole fusion (Merz and Wickner, 2004). The release of Ca^{2+} ions from the ER lumen was followed with the photoluminescent protein aequorin. During network formation, Ca^{2+} was released, reaching a maximum level of ~250 nM after 30 min (Figure 1B). At low salt concentrations, when larger vesicles form instead of networks, Ca^{2+} efflux was significantly slower. In the absence of GTP, Ca^{2+} efflux was negligible. These data show that network formation correlates with rapid Ca^{2+} efflux. Therefore, we have two assays that can be used to identify factors involved in ER tubule formation.

Identification of Reticulon 4a

Since all components required for in vitro ER network formation appeared to be tightly associated with membranes, we first searched for an inhibitor of the reaction and then identified its target. We found that very low concentrations ($\leq$5 μM) of various sulfhydryl (SH) reagents effectively inhibited network formation and, to some extent, vesicle fusion (Figure 1C). This effect could be prevented by the addition of dithiothreitol (DTT) (Figure 1C; lower right panel), indicating that inhibition is caused by the modification of an SH group in a protein involved in network formation. Since even large, membrane-impermeable SH reagents such as maleimide PEG (MP, 5 kDa) or maleimide neutravidin (MN, 60 kDa) block network formation (Figure 1C), the target SH group must be exposed on the cytoplasmic surface of the vesicles.

To identify the target, we used a biotinylation reagent. Membranes were modified with inhibitory concentrations (5 μM) of maleimide biotin and solubilized in detergent. The biotinylated proteins were bound to monomeric avidin agarose, eluted with excess biotin, and analyzed by SDS-PAGE, followed by staining with Coomassie blue (Figure 1D, lane 2; lane 3 shows a control in which modification was prevented by DTT). When an excess of the membrane-impermeable reagent maleimide PEG was added, several proteins were no longer biotinylated (Figure 1D, lane 4 versus lane 2). These proteins likely have a cytoplasmically exposed SH group and are thus the best candidates to be involved in ER network formation. Only three proteins showed this behavior. They were identified by mass spectroscopy as IP3 receptor 1 (IP3R; 300 kDa), reticulon 4a (Rtn4a/NogoA; runs at ~200 kDa), and reticulon 4b (Rtn4b/NogoB; 40 kDa).

Rtn4a/NogoA and Rtn4b/NogoB belong to the ubiquitous reticulon protein family, which are located in the ER (hence the name), and share a conserved C-terminal "reticulon domain" of ~190 amino acids that includes two hydrophobic segments (Oertle et al., 2003a; van de Velde et al., 1994). One of the reticulons, Rtn4a/NogoA has been implicated in inhibiting axon outgrowth because antibodies promote and soluble domains of Rtn4a/NogoA inhibit neurite growth (Chen et al., 2000; GrandPre et al., 2000; Oertle et al., 2003b). However, given that the reticulons are primarily localized to the ER (>95%) and have relatives in all eukaryotic cells, including yeast, it seems that they have intracellular and ubiquitous roles.

Rtn4a/NogoA Is Required for ER Network Formation In Vitro

To discriminate among the identified candidate proteins, we treated *Xenopus* membranes with increasing concentrations of maleimide biotin and analyzed modified proteins by blotting with peroxidase-coupled streptavidin (Figure 2A, upper panel). Only one band, corresponding in mobility to that of Rtn4a/NogoA, was seen, suggesting that the other proteins may be bound to the avidin beads via Rtn4a/NogoA, consistent with reported interactions among the reticulons (Dodd et al., 2005; Qi et al., 2003). Immunoblotting with antibodies raised against the common C terminus of Rtn4a/NogoA and Rtn4b/NogoB showed that, at a concentration of 5–10 μM maleimide biotin, Rtn4a/NogoA was quantitatively modified (second panel), correlating with complete inhibition of network formation (Figure 2B; results of visual assay in Figure 2C). On the other hand, Rtn4b/NogoB was only partially modified at even higher concentrations. These results suggest that Rtn4a/NogoA may be the major target of maleimide-biotin modification.

A role for Rtn4a/NogoA in network formation is further supported by modification experiments with the large reagent maleimide neutravidin. It selectively modified Rtn4a/NogoA, as indicated by the size shift in SDS-PAGE, but not Rtn4b/NogoB or IP3R (Figure 2D). The degree of modification of Rtn4a/NogoA correlated well with progressive

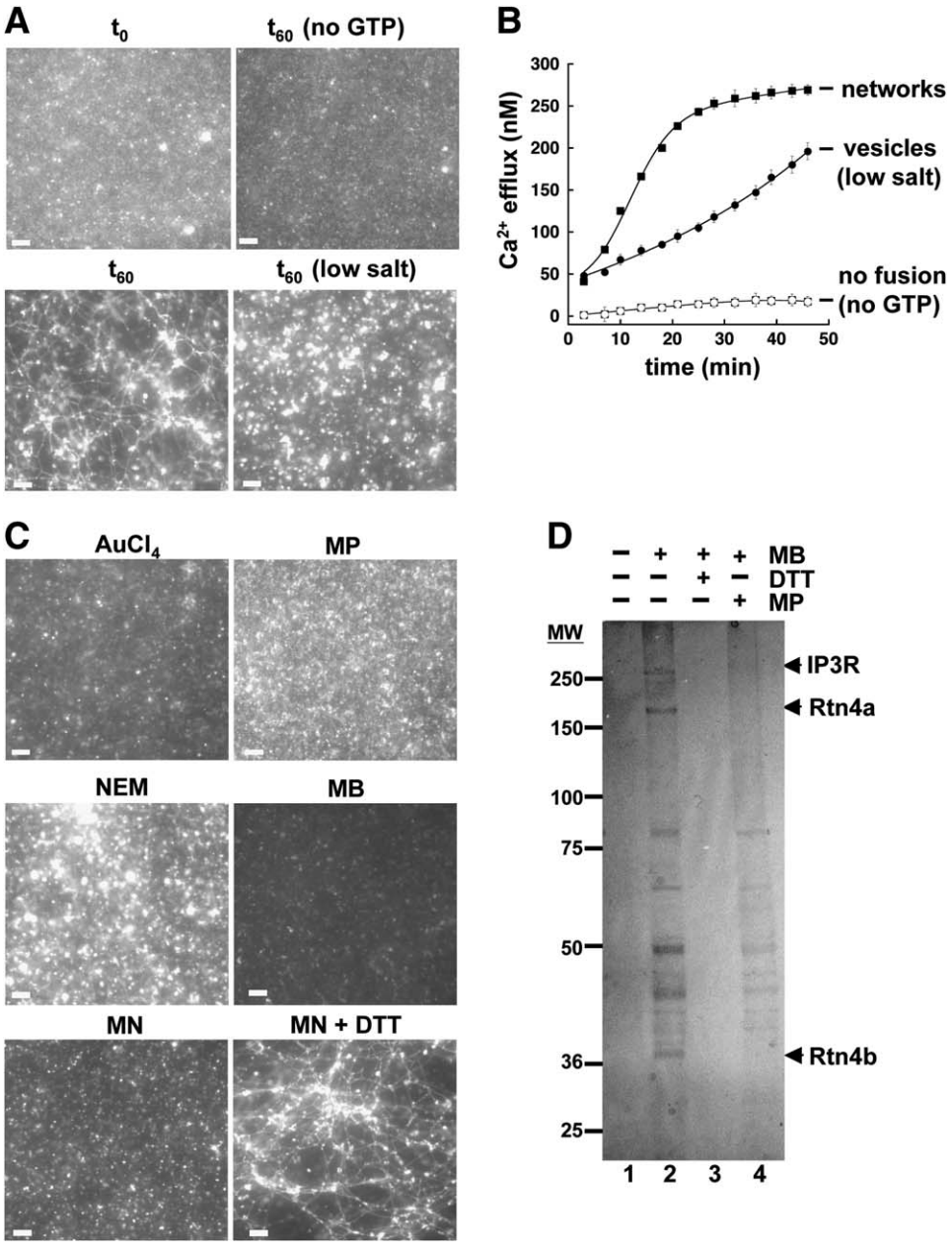

Figure 1. In Vitro ER Network Formation and the Effect of Sulfhydryl Reagents

(A) Salt-washed membranes from *Xenopus* eggs either were analyzed directly (t_0) or were incubated at 25ºC, 200 mM salt, and GTP for 60 min (t_{60}). Other samples were incubated at low salt (50 mM) or without GTP. All samples were stained with octadecyl rhodamine and visualized by fluorescence microscopy.

(B) Ca^{2+} efflux from membranes was measured with aequorin in a luminometer. The reaction was performed at 200 mM salt with GTP (networks), at low salt (50 mM) with GTP (large vesicles), or without GTP (at 200 mM salt; no fusion). Error bars represent standard deviation for three experiments.

(C) Washed membranes were preincubated for 20 min at 25ºC with 5 μM $AuCl_4$, maleimide PEG-5 kDa (MP), N-ethylmaleimide (NEM), or maleimide biotin (MB) or 1 μM maleimide neutravidin (MN). After addition of 1 mM DTT, the network formation reaction was performed at 200 mM salt with GTP. Where indicated, modification by MN was prevented with 1 mM DTT.

(D) Membranes were incubated with 5 μM MB for 20 min prior to addition of 1 mM DTT. Extracts in 1% Triton X-100 were incubated with monomeric avidin. Bound proteins were eluted with biotin and analyzed by SDS-PAGE and Coomassie staining. Where indicated, DTT (1 mM) or the membrane-impermeable reagent MP (50 μM) was added during biotinylation. Proteins modified only in the absence of MP were the IP3 receptor (IP3R) and two reticulons (Rtn4a/NogoA and Rtn4b/NogoB). Scale bar = 5 μm.

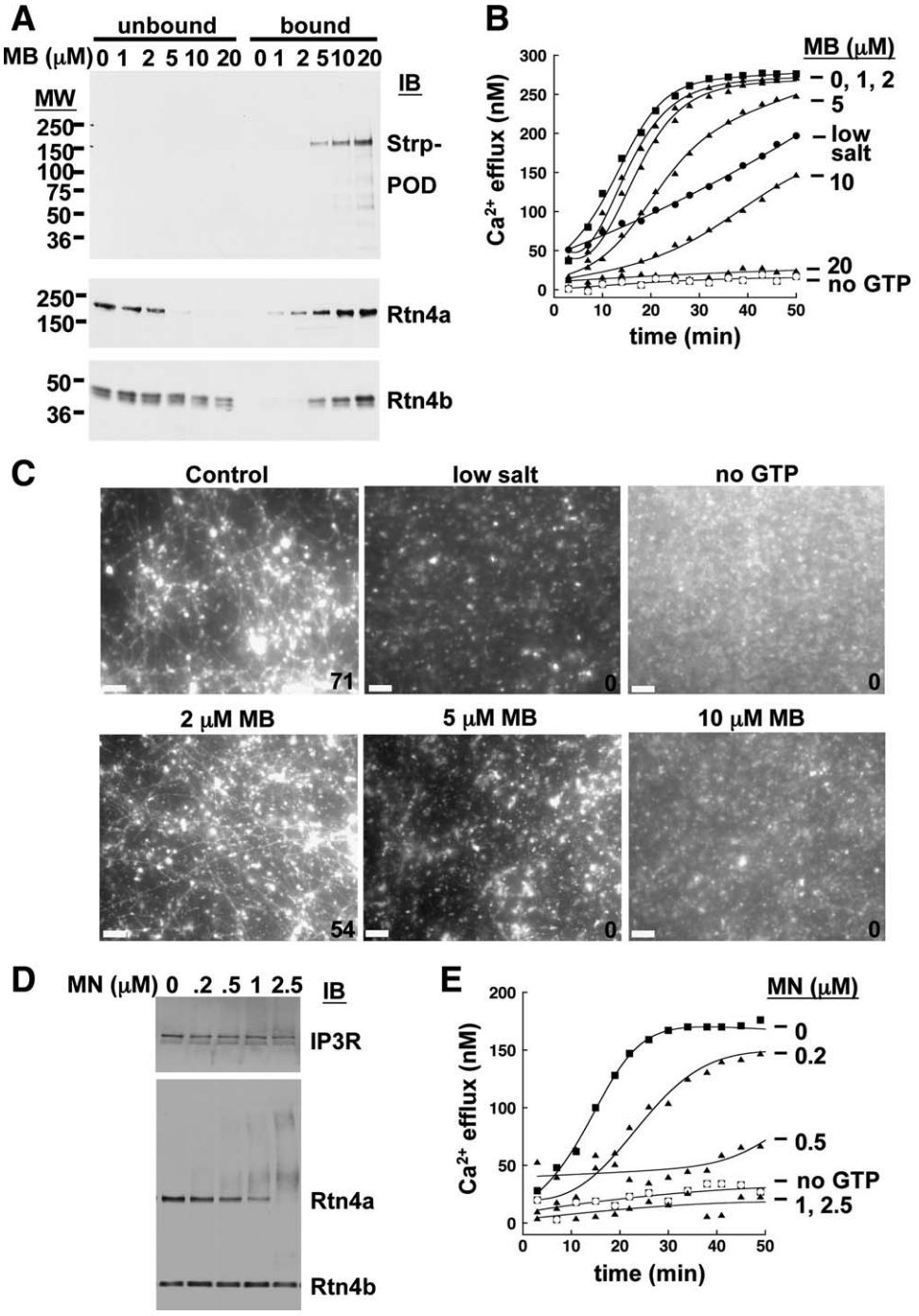

Figure 2. Rtn4a/NogoA Modification Correlates with Inhibition of Ca^{2+} Efflux

(A) Washed membranes were preincubated for 20 min with different concentrations of maleimide biotin (MB). The samples were treated with DTT, solubilized in Triton X-100, and incubated with monomeric avidin beads. Bound and unbound proteins were analyzed by SDS-PAGE and immunoblotting (IB) with peroxidase-coupled streptavidin (Strp-POD) or antibodies to Rtn4 C terminus.

(B) The reactions in (A) were tested for network formation by the Ca^{2+} efflux assay (no MB, filled squares; with MB, triangles). Controls were performed at low salt (vesicles formed, circles) or without GTP (no fusion, open squares).

(C) As in (B), except that network formation was tested visually. The number of three-way junctions in the networks is shown in the figures in the lower right corner.

(D) As in (A), except that modification was done with maleimide neutravidin (MN) and immunoblotting with antibodies to IP3 receptor (IP3R) and Rtn4.

(E) Reactions in (D) were tested in the Ca^{2+} efflux assay. Symbols as in (B).

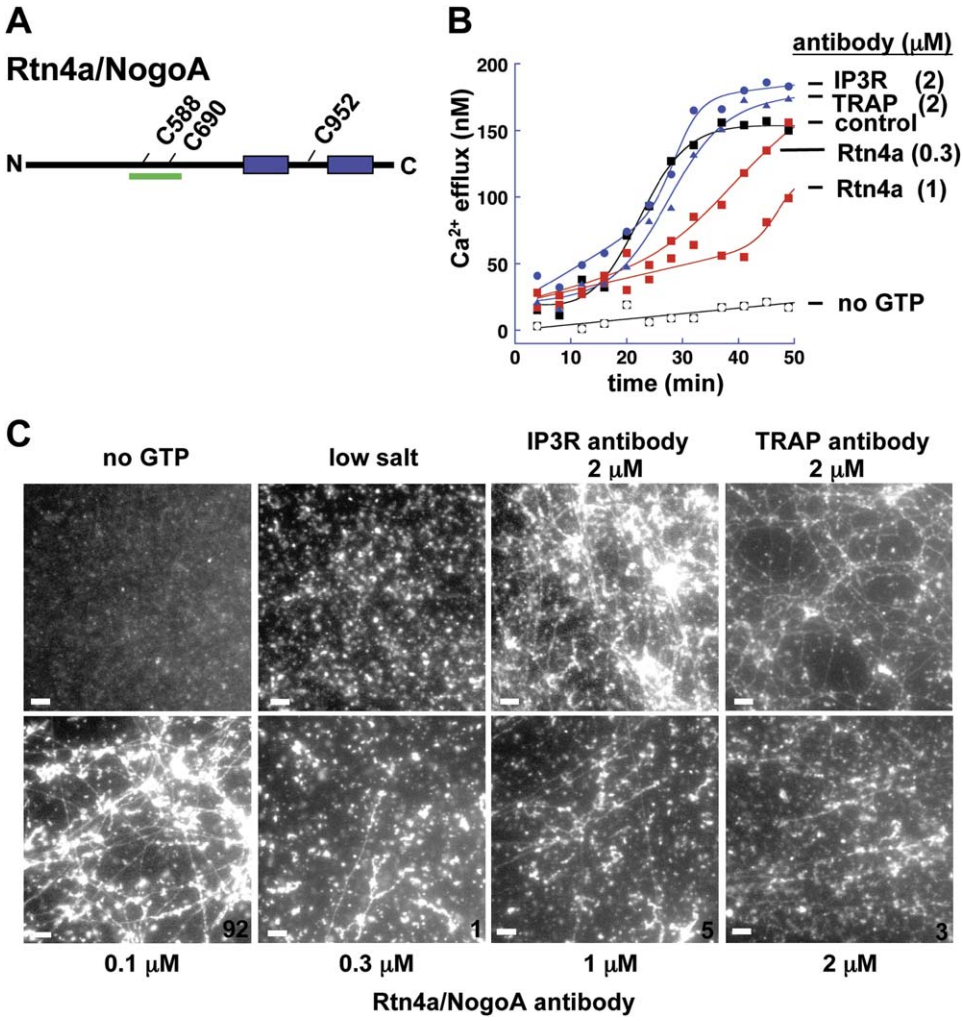

Figure 3. Antibodies to Rtn4a/NogoA Inhibit Network Formation

(A) Scheme of Rtn4a/NogoA. The two hydrophobic segments are shown in blue; the cysteines modified by N-ethylmaleimide are indicated; and the region 535–736, to which rabbit antibodies were raised, is shown in green.

(B) Different concentrations of affinity-purified antibodies were added to membranes for 60 min at 25ºC (Rtn4a/NogoA, red squares). In controls, antibodies to the C termini of the IP3 receptor 1 (IP3R, blue circles) or to TRAPα (blue triangles) were added. Network formation was initiated by the addition of GTP, and Ca^{2+} efflux was measured. A control reaction was performed without GTP (open squares).

(C) As in (B), except that network formation was tested visually. The number of three-way junctions in the networks is shown in the figures in the lower row. Control reactions were performed at low salt or without GTP. Scale bar = 5 μm.

inhibition of network formation, as followed by the Ca^{2+} efflux and visual assays (Figure 2E and data not shown). Similar results were obtained with the reagent maleimide PEG (data not shown).

To further test whether Rtn4a/NogoA is a key component involved in ER network formation, we wished to raise inhibitory antibodies. We reasoned that a good target for antibodies might be an Rtn4a/NogoA domain that contains cysteines modified by inhibitory concentrations of the SH reagents. We identified by mass spectrometry cysteines modified by N-ethylmaleimide and found two of them in the N-terminal domain of Rtn4a/NogoA (Figure 3A), which is located in the cytosol (Oertle et al., 2003a; see also below) and is lacking in Rtn4b/NogoB. Antibodies raised against a segment (positions 535–736) that includes these two cysteines were affinity purified and recognized a major protein of the expected size (Figure S2). When preincubated with membrane vesicles, they inhibited network formation as measured by Ca^{2+} efflux; inhibition was seen at concentrations as low as 0.3 μM (Figure 3B). Similar results were seen in the visual assay (Figure 3C). Interestingly, although few networks were generated at high antibody concentrations, vesicle fusion was still observed (Figure 3C, compare with low salt panel). The antibodies also did not block fusion into large vesicles at low salt concentrations, although a slight inhibition cannot be excluded (Figure S3). Inhibition of

network formation, but not fusion, was also seen with a crude IgG fraction prepared from the Rtn4a/NogoA antiserum, while IgG depleted of Rtn4a/NogoA antibodies had no effect (Figure S4). On the other hand, even high concentrations of affinity-purified antibodies to the abundant ER membrane proteins IP3R or TRAPα did not inhibit network formation as measured by the Ca^{2+} efflux (Figure 3B) or visual (Figure 3C) assays. These data thus indicate that Rtn4a/NogoA is required for ER network formation in vitro.

Exclusive Localization of the Reticulons to the Tubular ER

If Rtn4a/NogoA plays a role in ER tubule formation or maintenance, one might expect it to localize specifically to the tubular ER. We first tested the localization of mammalian Rtn4a/NogoA in COS cells. Cells transiently expressing Myc-tagged Rtn4a/NogoA together with a GFP fusion to Sec61β were analyzed by fluorescence microscopy (Figure 4A). While Sec61β showed the typical distribution of an ER protein to both the nuclear envelope and the reticular network, Rtn4a/NogoA was prominent in the peripheral ER and essentially absent from the nuclear rim (upper panels). When the microscope was focused on the peripheral ER, the nucleus appeared bright when analyzed for Sec61β and dark when stained for Rtn4a/NogoA (lower panels). A similar, almost exclusive distribution to the peripheral ER was seen for Rtn4c/NogoC, a reticulon isoform that essentially contains only the reticulon domain (Figure 4B). Even in cells that overexpressed Rtn4a/NogoA or Rtn4c/NogoC, a nuclear-envelope localization was not observed. Rtn4c/NogoC was also depleted from Sec61β-containing membrane sheets (cisternae) of the peripheral ER (Figure 4B, merged image in lower panel), and Rtn4a/NogoA expression appears to abolish peripheral ER sheets (Figures 5A and 5B; see also below). The reticulons are the first proteins specifically localized to the tubular ER. The only other known ER protein that is excluded from the nuclear envelope is CLIMP-63, a single-spanning membrane protein found in higher eukaryotes (Klopfenstein et al., 2001; Schweizer et al., 1995), but it is found in peripheral ER sheets (unpublished data).

We next tested the localization of the two reticulons in *S. cerevisiae*, Rtn1p and Rtn2p, using GFP fusions expressed under the endogenous promoters. Both Rtn1p-GFP and Rtn2p-GFP were almost absent from the nuclear envelope, whereas they were abundant in the tubules of the peripheral ER (Figure 4B). The peculiar localization of Rtn1p was also seen in a recent study, although at higher expression levels, some nuclear localization was reported (Geng et al., 2005). GFP fusions to six other abundant ER membrane proteins (Sec63p, Figure 4B, upper panels; Erp2p, Sur2p, Wbp1p, Ost1p, and Erg3p, data not shown), were localized to both the nuclear and peripheral ER. The different localizations were confirmed by the analysis of cells that expressed a reticulon together with Sec63p (Figure S5).

An exclusive localization to the peripheral, tubular ER was also observed for endogenous Rtn4 in *Xenopus* tissue culture cells (Figure S6) and for a GFP fusion to *Drosophila* Rtn1 expressed under the endogenous promoter (M. Rolls, personal communication). Together, these results show that the reticulons are restricted to the tubular, peripheral ER, consistent with a role in shaping this organelle.

ER Structure Changes on Reticulon Overexpression or Deletion

The role of the reticulons in forming ER tubules is supported by ER morphology changes observed upon overexpression of Rtn4a/NogoA-Myc in COS cells. The ER tubules were generally longer and less branched (Figure 5A, compare with upper left control panel). Membrane sheets in the peripheral ER, which are normally seen when cells express only GFP-Sec61β, were essentially absent (for quantitation, see Figure 5B). Almost every Rtn4a/NogoA-expressing cell had one or more long process that contained parallel or bundled ER tubules (Figure 4A, boxed area; Figure 5A, lower panels; quantitation in Figure 5B). Rtn4a/NogoA-Myc localized all the way to the periphery of the cell, whereas GFP-Sec61β was concentrated close to the nucleus (Figure 4A, lower panel, merge; for quantitation of the effect, see Figure S7), suggesting that Rtn4a/NogoA displaces Sec61β from the peripheral ER.

Similar results were obtained in *S. cerevisiae*. Expression of hemagglutinin (HA) tagged Rtn1p under an inducible Gal promoter resulted in disruption of the peripheral ER but left the nuclear envelope intact (Figure 5C). Rtn1p-GFP was often localized to long filaments (top panel), which were not seen with the other ER proteins. The overexpression of a control ER protein (Erg3p) under the same Gal promoter did not result in long filaments (Figure 5C, lower left panels; similar data for Ost1p not shown). These structures are distinct from karmellae formed by the overexpression of some ER proteins (e.g., Hmg2p; see Figure 5C, lower right panel). These data suggest that, in both mammalian and yeast cells, the reticulons have a strong preference to localize to the tubular ER. When overexpressed, the reticulons even appear to induce tubules (Figures 5A and 5C).

Next we tested whether yeast cells lacking the reticulons have altered ER morphology. Mutants lacking Rtn1p, Rtn2p, or both are viable, and, even in the double-deletion mutant, the morphology of the peripheral ER network appeared normal (data not shown). However, when the cells were placed for 1 hr in a high-osmolarity medium (1 M NaCl [Figure 5D] or 1 M sorbitol [data not shown]), the peripheral ER converted into membrane sheets (Figure 5D, lower right panel). This effect was not seen with the wild-type strain or the single-deletion mutants (Figure 5D and data not shown). Therefore, the reticulons are needed for the maintenance of tubular ER under certain stress conditions, but they cannot be the only components required under normal circumstances.

A Reticulon-Interacting Protein

Given that the reticulons associate with one another, we reasoned that additional components involved in shaping the tubular ER might be found in a complex with them. We therefore searched for partners of *Xenopus* Rtn4a/NogoA either

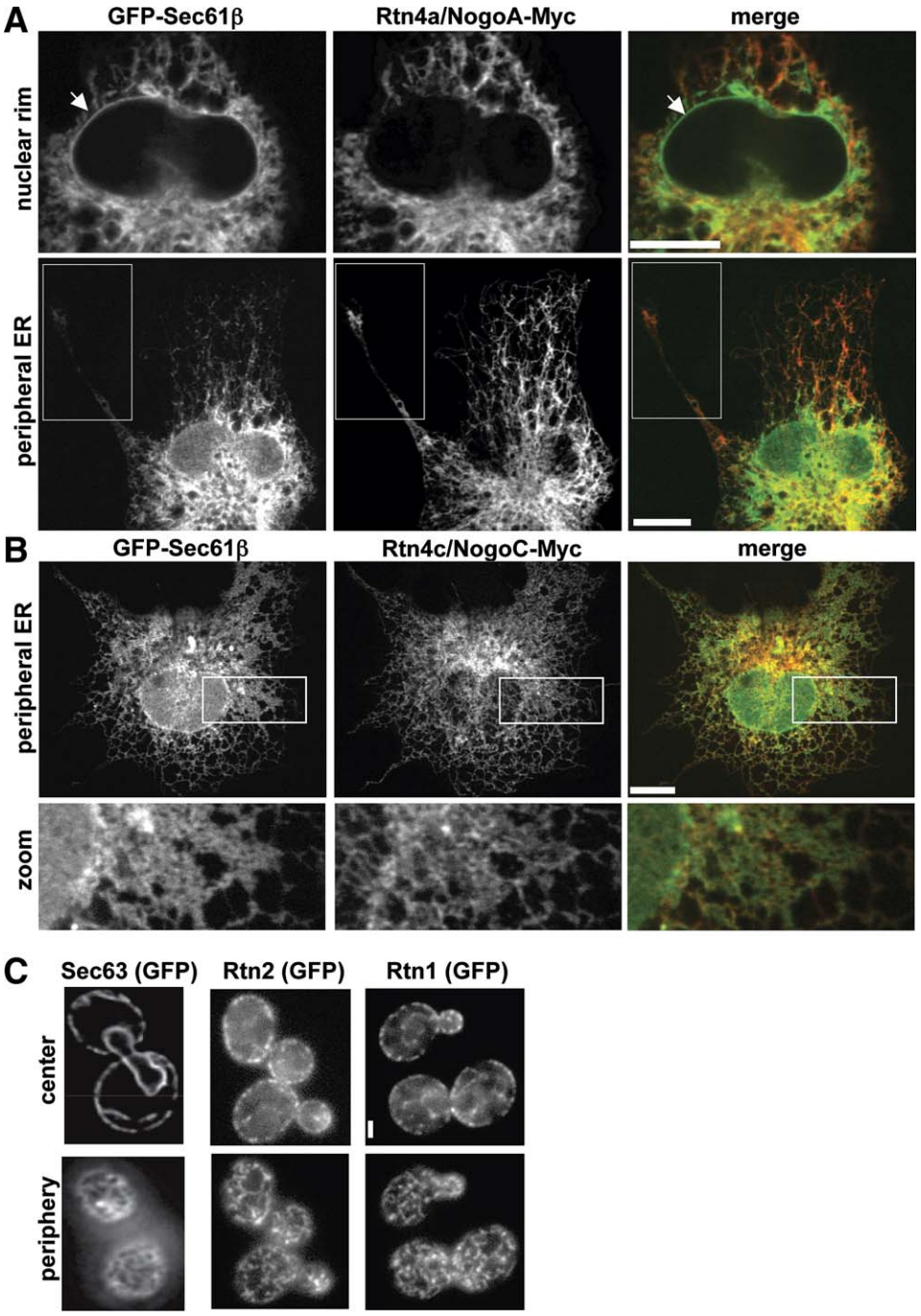

Figure 4. Localization of the Reticulons

(A) COS cells coexpressing Myc-tagged rat Rtn4a/NogoA (Rtn4a/NogoA-Myc) and a GFP fusion to Sec61β (GFP-Sec61β) were analyzed with a confocal fluorescence microscope (Myc, red; GFP, green). The right panels show merged images. The microscope was focused on either the plane of the nuclear rim (upper panels; white arrows point to the rim) or the peripheral ER (lower panels). Boxes highlight tubular protrusions seen upon overexpression of Rtn4a/NogoA.

(B) The upper three panels show COS cells coexpressing Myc-tagged rat Rtn4c/NogoC (Rtn4c/NogoC-Myc) and GFP-Sec61β. The lower three panels show an enlargement of the boxed region.

(C) Yeast cells expressing GFP fusions to Sec63p, Rtn1p, or Rtn2p under the endogenous promoters were visualized by fluorescence microscopy. The microscope was focused on the center or periphery of the cells. Scale bars in (A) and (B) = 10 μm; (C) = 1 μm.

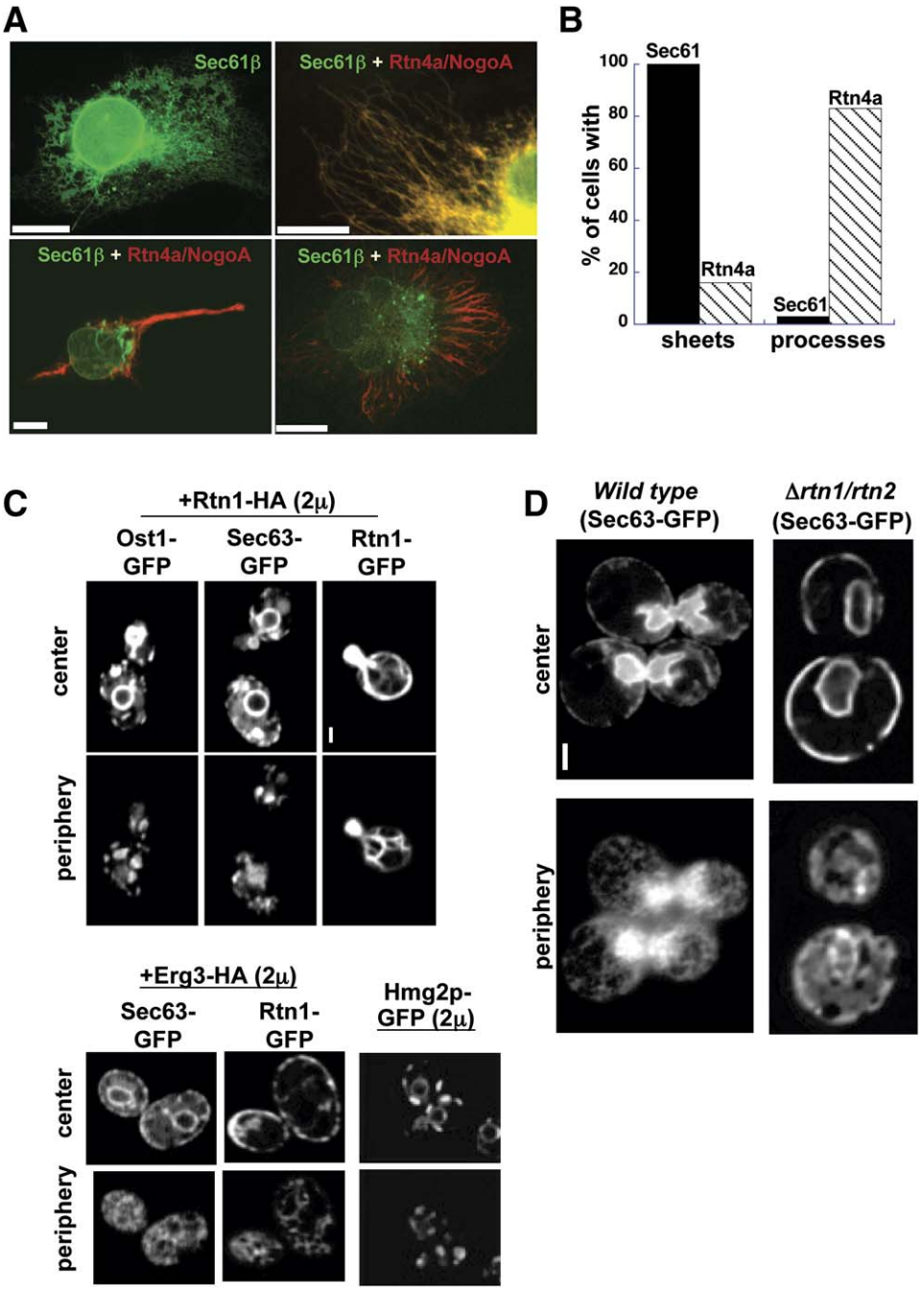

Figure 5. Overexpression and Deletion of the Reticulons

(A) A COS cell with normal ER, expressing only GFP-Sec61β, and examples of cells expressing both Rtn4a/NogoA-Myc (red) and GFP-Sec61β (green).

(B) Percent of cells with ER sheets or long processes when expressing Sec61β or Rtn4a/NogoA; n = 30 cells.

(C) Localization of GFP-fusions to Rtn1p, Sec63p, or Ost1p in yeast strains expressing HA-tagged Rtn1p (Rtn1-HA) or Erg3p (Erg3-HA) under the Gal promoter. The cells were analyzed by fluorescence microscopy before and after induction of expression for 2 hr, focusing at either the center or periphery. The lower right panel shows the appearance of karmellae in cells overexpressing a GFP fusion to HMG-CoA reductase 2 (Hmg2p).

(D) Localization of a GFP fusion to Sec63p in wild-type or Δ*rtn1*/Δ*rtn2* cells. The cells were grown for 1 hr in medium containing 1 M NaCl and were visualized by fluorescence microscopy. Scale bars in (A) = 10 μm; (C) and (D) = 1 μm.

by precipitating Rtn4a/NogoA from membrane extracts using affinity-purified antibodies to its N terminus or by first modifying Rtn4a/NogoA in membranes with maleimide neutravidin and then incubating the extract with biotin beads. With both approaches, mass spectrometry identified an integral, ubiquitous membrane protein, called DP1 (for ''deleted

in polyposis'') or TB2 (Joslyn et al., 1991) (Figure 6A; Figure S8). In addition, Rtn3 was found, consistent with the previously reported interactions among the mammalian reticulons (Dodd et al., 2005; Qi et al., 2003). An association between the yeast reticulons and the DP1 homolog Yop1p (Calero et al., 2001) could also be demonstrated; when TAP-tagged Yop1p was expressed under its endogenous promoter and purified on IgG beads, HA-tagged Rtn1p or Rtn2p expressed in the same cells was copurified (Figure 6B). TAP-tagged Rtn1p also interacted with Rtn1p-HA or Rtn2p-HA (Figure 6B), demonstrating that the reticulons form homo- and hetero-oligomers in yeast. Rtn1p is one of the most abundant membrane proteins (~37,000 molecules/cell) (Ghaemmaghami et al., 2003), and Yop1p appears to be equally abundant as judged from immunoblots of the TAP-tagged proteins expressed under the endogenous promoters (data not shown). Rtn2p seems to be significantly less abundant (unpublished data and http://yeastgfp.ucsf.edu).

Like the reticulons, HA-tagged DP1 localized exclusively to the tubular ER in COS cells, avoiding both the nuclear envelope and peripheral ER sheets (Figure 6C). In cells expressing HA-DP1 and Rtn4a/NogoA-Myc, the tagged proteins colocalized (Figure 6D). DP1 did not overflow into the nuclear membranes when overexpressed. Similarly, in *S. cerevisiae*, Yop1p-GFP was found in the peripheral ER but was essentially absent from the nuclear envelope (Figure 6E).

Finally, we tested whether Yop1p is the missing component for maintaining peripheral ER morphology in *S. cerevisiae*. Indeed, cells lacking both reticulons and Yop1p had disrupted peripheral ER under normal growth conditions, while the nuclear envelope appeared to be unaffected (Figure 6F). The peripheral ER appeared as sheets, but occasionally some peripheral tubules could be seen, suggesting that there may be yet another, minor component contributing to ER shape. The triple-knockout mutant grew at about 2/3 the rate of wild-type cells. The ER morphology defects are not caused by a block of vesicular trafficking out of the ER because carboxypeptidase Y was processed normally from the ER—via the Golgi—to the vacuole form (Figure S9). ER morphology defects similar to those in the triple mutant were also seen in mutants lacking Rtn1p and Yop1p (Figure 6F). In contrast, the ER appeared similar to wild-type in mutants lacking Rtn2p and Yop1p (Figure 6F), although ~10% of the cells showed peripheral ER sheets. Since Rtn1p and Yop1p are significantly more abundant than Rtn2p, these data suggest that they are the major, redundant components required to maintain the tubular ER under normal circumstances.

The Reticulons and DP1/Yop1p Form a Hairpin

The peculiar, almost exclusive localization of the reticulons and DP1/Yop1p to the tubular ER, as well as the fact that these proteins each have two hydrophobic segments of unusual length (~30–35 residues; normal length is ~20), prompted us to determine their membrane topology with a new and simple method. We introduced single cysteines into the three hydrophilic segments of wild-type Rtn4c/NogoC-Myc, which has no cysteines, and expressed the mutant proteins in COS cells (Figure 7A). A low concentration of digitonin was added to permeabilize the plasma membrane but not the ER (Le Gall et al., 2004). The membrane-impermeable reagent maleimide PEG (5 kDa) was then added, and the modification of the proteins was tested by their molecular-weight shift in SDS gels (Le Gall et al., 2004). The cysteines in the N-terminal domain and in the segment between the hydrophobic sequences were readily modified, in contrast to the ER-luminal protein Grp94 (Figure 7A, lanes 2 and 3). Controls showed that modification was blocked by DTT (lanes 6–10) and that all proteins were modified when the ER membrane was permeabilized with Triton X-100 (lanes 11–15). These data show that the first hydrophobic segment adopts a hairpin structure in the membrane. The second hydrophobic segment may also form a hairpin, but its topology is less certain because the C-terminal cysteine was only partially modified (lane 4). Similar experiments were performed with HA-DP1, except that individual cysteines in the different domains were mutated to alanines or a cysteine was inserted (Figure 7B). Mutation of the cysteine in the N-terminal domain resulted in the loss of modification (Figure 7B, lane 2 versus lane 1), while insertion of a cysteine into the segment between the hydrophobic segments resulted in an additional modification (lane 5). Thus, the first hydrophobic segment again forms a hairpin in the membrane. The topology of the second segment remains uncertain. Together, these results show that the reticulons and DP1/Yop1p share a rather unusual membrane topology of at least their first hydrophobic segment.

DISCUSSION

By identifying the major components required to shape the tubular ER, our results provide insight into how the characteristic structure of an organelle is generated. First, based on the inhibitory effect of sulfhydryl reagents and antibodies, we show that Rtn4a/NogoA is required for ER tubule formation in vitro. Second, we find that the reticulons and DP1/Yop1p localize almost exclusively to the tubular ER, a unique localization that is consistent with a role in shaping this ER domain, in both mammalian and yeast cells. These proteins avoid not only the sheets of the nuclear envelope but also those in the peripheral ER. Third, the overexpression of the reticulons both in mammalian and yeast cells leads to long, relatively unbranched, and often bundled tubules. The overexpression of Rtn4a/NogoA in COS cells further abolishes peripheral ER sheets and leads to long cellular processes containing tubular ER. Finally, the deletion of the reticulons in yeast leads to the disruption of the peripheral tubular ER in stress situations, and the additional deletion of Yop1p leads to similar ER morphology defects under normal growth conditions. Together, these results indicate that the reticulons and DP1/Yop1p are ''morphogenic'' proteins that are necessary to form and maintain the tubular ER.

How could the reticulons and DP1/Yop1p shape ER tubules? A major difference between ER tubules and the sheets of the nuclear envelope and peripheral ER is that

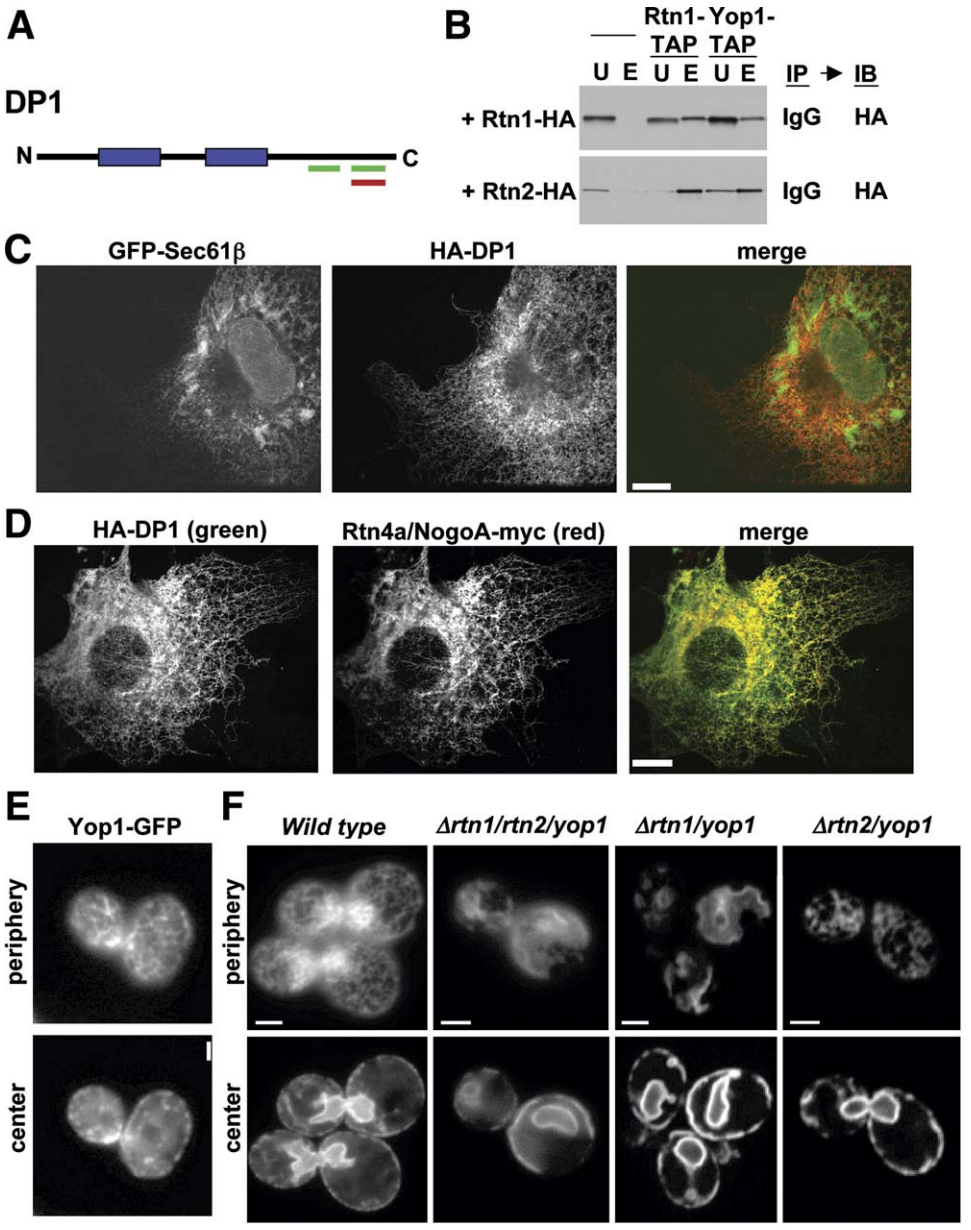

Figure 6. A Role for the Reticulon-Interacting Protein DP1/Yop1p in ER Tubule Formation

(A) A *Xenopus* Rtn4a/NogoA-interacting protein (DP1) was identified by pulling on Rtn4a/NogoA either with antibodies followed by protein A beads or with biotin beads after maleimide-neutravidin modification of membranes. Peptides identified by mass spectrometry are indicated in green and red, respectively (sequences in Figure S8). Hydrophobic segments are shown in blue.

(B) TAP-tagged Rtn1p or Yop1p, the homolog of DP1, was expressed in yeast under the endogenous promoters, and HA-tagged Rtn1p or Rtn2p was expressed from a CEN plasmid. TAP-tagged proteins were bound to IgG beads, and SDS-eluted (E) and unbound (U) proteins were analyzed by SDS-PAGE and immunoblotting (IB) with HA antibodies. A control was performed with cells lacking TAP-tagged proteins.

(C) COS cells expressing GFP-Sec61β (green) and HA-DP1 (red) were analyzed by confocal fluorescence microscopy. The right panel shows a merged image.

(D) COS cells expressing HA-tagged DP1 (HA-DP1, green) and Myc-tagged Rtn4a (Rtn4a-Myc, red) were analyzed by confocal fluorescence microscopy.

(E) Yeast cells expressing Yop1p-GFP under the endogenous promoter were analyzed by fluorescence microscopy, focusing at either the center or periphery.

(F) A GFP fusion to Sec63p was visualized in yeast wild-type and Δ*rtn1*/Δ*rtn2*/Δ*yop1*, Δ*rtn1*/Δ*yop1*, and Δ*rtn2*/Δ*yop1* cells. Scale bars in (C) and (D) = 10 μm; (E) and (F) = 1 μm.

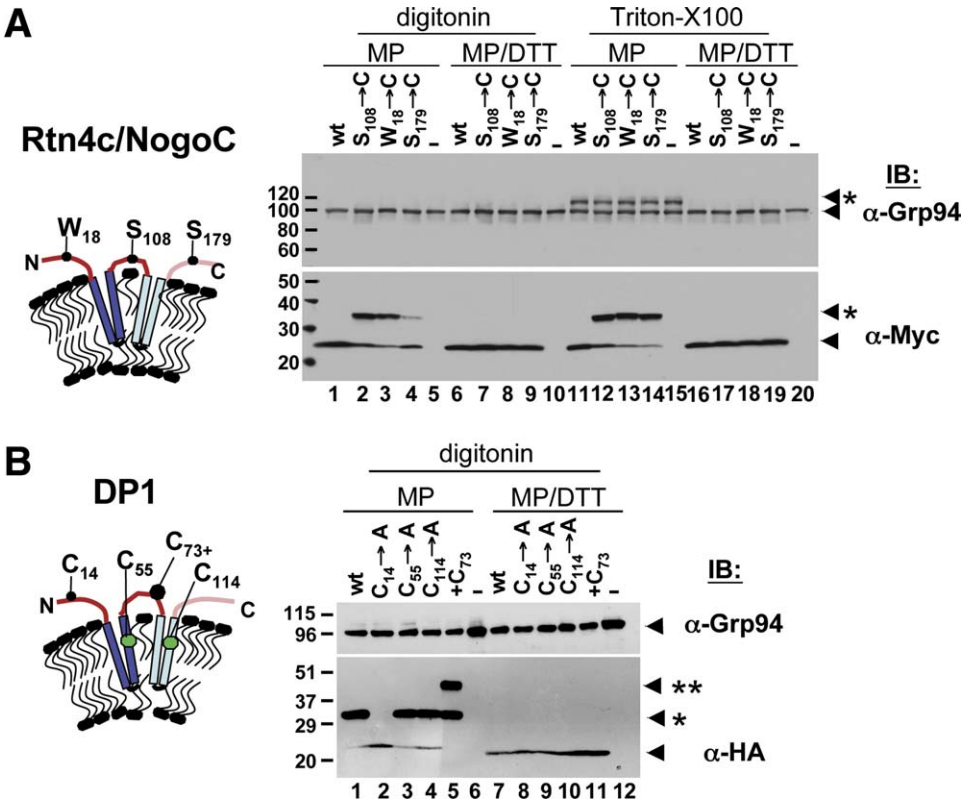

Figure 7. Membrane Topologies of Rtn4c/NogoC and DP1 Determined by Cysteine Modification

(A) Single cysteines were placed at the indicated positions into the three hydrophilic domains of wild-type (wt) Rtn4c/NogoC, which lacks cysteines. Myc-tagged Rtn4c/NogoC mutants or wt were expressed in COS cells. Digitonin or Triton was added, followed by maleimide PEG 5 kDa (MP) in the absence or presence of DTT. SDS-PAGE was performed, followed by immunoblotting with Myc antibodies. The luminal ER protein Grp94 served as control. A control was done without transfection (–). Light blue and red indicate uncertain topology. Stars indicate the number of MP molecules added to the proteins.

(B) As in (A), except individual cysteines in HA-tagged wild-type DP1 were mutated to alanines or a cysteine was inserted ($+C_{73}$).

tubules have a high curvature in cross-section. The reticulons and DP1/Yop1p may function to stabilize such high-curvature membranes, an otherwise energetically unfavorable state, explaining why they would be necessary for the generation of tubular ER. Conversely, if the reticulons and DP1/Yop1p partitioned into membranes with a high curvature, this would explain their localization to the tubular ER; they would avoid the low-curvature sheets of the nuclear envelope and peripheral ER. It is indeed difficult to think of another mechanism of localization, such as the binding to another component, because each of these proteins maintains its localization even when highly expressed.

The stabilization of high-curvature membranes might also explain the role of Rtn4a/NogoA in ER network formation in vitro. The starting, small vesicles have a high curvature, and, when they fuse, Rtn4a/NogoA might exert a structural constraint that would maintain high curvature and prevent the expansion into a larger vesicle with lower curvature. Consistent with this model, the addition of antibodies to Rtn4a/NogoA leads to larger vesicles rather than ER tubules. How exactly the antibodies and sulfhydryl reagents affect Rtn4a/NogoA remains to be clarified. Given the redundancy of the reticulons and DP1/Yop1p in yeast, it is somewhat surprising that Rtn4a/NogoA plays such a major role in ER tubule formation in vitro. Perhaps, the de novo formation of ER tubules from small vesicles is more demanding, or the reagents exert a dominant-negative effect. For example, modification of the N terminus of Rtn4a/NogoA may disturb the function of DP1, Rtn4b/NogoB, and Rtn3 as well since these are all in one complex. In vitro network formation requires GTP-dependent vesicle fusion, which appears to involve different components since antibodies to Rtn4a/NogoA inhibit only network formation and the reticulons are not predicted to be nucleotide binding proteins. Nevertheless, it is possible that Rtn4a is associated with the fusion machinery because sulfhydryl reagents inhibit fusion at only slightly higher concentrations than network formation. Other aspects of the in vitro reaction, such as the effect of salt and the role of Ca^{2+} efflux, also require further study.

What features of the reticulons and DP1/Yop1p could be responsible for their ability to generate tubules of high curvature? It is useful to consider the analogy with vesicle budding, in which initial membrane curvature is generated by the action of cytosolic proteins, such as endophilin, amphiphysin, epsin, Sar1p, and probably Arf1p. These proteins cause curvature by inserting an amphipathic helix into the outer leaflet

of the lipid bilayer. In addition, several protein molecules need to cluster at the site of membrane deformation (for review, see Farsad and De Camilli, 2003; Lee et al., 2005). Since the budded vesicle must fuse with a target membrane, the induced curvature is reversible and transient.

In the case of ER tubule formation, the mechanism by which curvature is induced might be similar, but membrane deformation would not be transient. The important region of the reticulons and DP1/Yop1p probably comprises the two hydrophobic segments because Rtn4c/NogoC, which only contains this domain, exclusively localizes to the reticular ER. One possibility is that this region adopts a wedge shape, occupying more space in the outer than the inner leaflet of the lipid bilayer (Chou et al., 2001). This structure might be caused by the unusual topology that we determined for one of the two hydrophobic segments in these proteins: a hairpin inside the membrane. In addition, as in vesicle budding, clustering of the proteins may be important to generate curvature over a sizable distance, consistent with the observation that the reticulons associate with one another and with DP1/Yop1p. A high concentration of the proteins in the ER appears to be important for large-scale tubulation because the simultaneous absence of the abundant Rtn1p and Yop1p results in ER morphology defects in yeast, demonstrating that they have redundant functions despite the fact that they are not sequence related. In contrast, the absence of the Rtn1p homolog Rtn2p has little effect, likely because it is significantly less abundant. In the absence of Yop1p, ER tubules can be maintained by Rtn1p alone, probably because Rtn1p can form oligomers on its own. The reticulons and DP1/Yop1p may be similar to caveolin, an integral membrane protein that forms oligomers and is abundant in and required for the formation of curved invaginations of the plasma membrane, called caveoli (for review, see Parton and Richards, 2003). Caveolin contains a single hydrophobic segment of ~34 residues, which sits in the membrane as a hairpin (Ostermeyer et al., 2004), similar to the first hydrophobic segment of the reticulons and DP1/Yop1p. Despite the attractive analogy to vesicle budding, other models for how the reticulons and DP1/Yop1p generate ER tubules and partition into them cannot be excluded. In the case of Rtn4a/NogoA, the N-terminal, cytoplasmic domain may also be important for its function in ER tubule formation because its modification with SH reagents or interaction with antibodies inhibit network formation in vitro. A detailed analysis of the significance of the hairpin structure of the hydrophobic segments and of the cytoplasmic domains is required to identify signals that target the reticulons and DP1/Yop1p to the tubular ER.

In mammals, there are many isoforms of the reticulons, which differ greatly at their N termini (Oertle and Schwab, 2003). These variable domains are likely to interact with distinct proteins and might link the reticulons to functions different from their role in ER tubule formation. Several interaction partners of the reticulons have been reported, but, surprisingly, most of them reside in compartments outside the ER. These include plasma-membrane-localized AP-2, endosomal Rme-1 and SNAREs, and mitochondrial Bcl-2, all found in two-hybrid screens (Iwahashi and Hamada, 2003; Iwahashi et al., 2002; Steiner et al., 2004; Tagami et al., 2000), as well as Golgi-localized Yip3p, detected in coprecipitation experiments (Geng et al., 2005). Perhaps, a small percentage of the reticulons acts in other cellular compartments, as has been reported for Rtn4a/NogoA acting on the plasma membrane to inhibit neurite outgrowth (Chen et al., 2000; GrandPre et al., 2000; Oertle et al., 2003b). Alternatively, the reticulons might link the ER to other organelles. A connection with vesicular trafficking out of the ER is also possible, since a subpopulation of Yop1p in *S. cerevisiae* interacts with Yip1p (Calero et al., 2001), a component of the Yip1p/Yif1p/Yos1p complex that appears to be involved in vesicle formation (Heidtman et al., 2005), and the overexpression of Yop1p has a mild trafficking defect (Calero et al., 2001). However, the reticulons and DP1/Yop1p have a direct effect on ER shape, independent of a possible role in trafficking, because yeast cells lacking the Rtns and Yop1p grow normally and have no secretion defect. In addition, the reticulons are abundant in the ER of neurites, where probably few, if any, transport vesicles are formed, and Rtn4a/NogoA has a role in ER tubule formation in vitro. In mammalian tissues, the various reticulon isoforms are prominent in different tissues, and some cells have low expression levels of all tested reticulons (Oertle and Schwab, 2003). While it is possible that low reticulon levels are compensated for by high DP1 expression, these differences could also reflect the fact that some cells, particularly those specialized in secretion, have extensive ER sheets rather than tubules. We have also observed that the overexpression of Rtn4a/NogoA in COS cells leads to long processes, raising the intriguing possibility that there might be a connection with the cytoskeleton and perhaps even with the formation of neurites in neuronal cells. Our results pave the way to an answer to these interesting questions.

EXPERIMENTAL PROCEDURES

Constructs

Rtn4a/NogoA (human) and Rtn4c/NogoC (rat), tagged with the Myc epitope at their C termini, were described previously (GrandPre et al., 2000). A GFP fusion to Sec61β was PCR amplified from a previously described construct (VLP25) (Rolls et al., 1999) and inserted into pcDNA3.1 vector using the TOPO cloning technology (Invitrogen). DP1 was PCR amplified from mouse cDNA, N-terminally HA tagged, and inserted into pcDNA3.1. For antibody production, GST fusions to *Xenopus* IP3R-1 or Rtn4a/NogoA were generated by PCR, amplifying the coding regions from a *Xenopus* cDNA library and cloning into pGEX4T2.

S. cerevisiae Strains and Plasmids

Strains expressing GFP fusions to various proteins were purchased from Invitrogen. The following strains were also used: BY4741 (*MAT***a** *his3Δ1 leu2Δ met15Δ ura3Δ*), WPY787 (BY4741 *rtn1::kanMX4 rtn2::kanMX4*), NDY256 (BY4741 *rtn1::kanMX4 yop1::kanMX4*), NDY257 (NDY256 *rtn2::kanMX4*), and NDY 259.5 (BY4741 *rtn2::kanMX4 yop1::kanMX4*). The plasmid encoding red fluorescent protein (RFP) fused to the C terminus of Sec63p (pND9) was constructed by cloning RFP from pRSETB (Invitrogen) into pJK59 (Prinz et al., 2000) between XhoI and HindIII sites. To generate yeast expression constructs, the coding regions of Rtn1p, Erg3p, and Ost1p were PCR amplified from wild-type yeast DNA using

a 3′ primer encoding an in-frame HA tag and cloned into the BamHI/XhoI site of pESC-URA (2μ) or pYC2-URA (CEN).

S. cerevisiae cells were imaged live in growth medium at room temperature using an Olympus BX61 microscope, UPlanApo 100×/1.35 lens, QImaging Retiga EX camera, and IPabs version 3.6.3 software. The pictures in Figure 5C (with the exception of Erg3-HA expression) and Figure 6F were taken with a confocal microscope (a Nikon Eclipse E800 microscope equipped with a PerkinElmer Ultraview LCI CSU10 scanning unit [PerkinElmer, Freemont, CA], an argon/krypton ion laser [Melles Griot, Carlsbad, CA], and an ORCA ER cooled CCD camera [Hamamatsu, Japan]). Image acquisition, analysis, and processing were done with Openlab 3 software (Improvision, Lexington, MA).

Expression in COS Cells

Transfection of DNA into COS cells was performed using Lipofectamine 2000 (Invitrogen). The cells were split 24 hr after transfection onto acid-washed coverslips and allowed to grow and spread for an additional 24 hr. For immunofluorescence microscopy, cells were fixed with 4% paraformaldehyde (EMS) in PBS, permeabilized in 0.1% Triton X-100 (Pierce), and stained with antibodies to Myc (mAb9E10; Santa Cruz) at 1:1000 dilution or to HA (rat 3F10, Roche) at 1:200 dilution, followed by Alexa 568-conjugated anti-mouse IgG or anti-rat IgG (Molecular Probes), both in 10% calf serum.

Antibodies and Proteins

Peptide antibodies to the C terminus of *Xenopus* Rtn4 (positions 1023-1043) were produced in rabbits by Zymed. Antibodies to IP3R-1 (amino acids 2535–2693) and Rtn4a (amino acids 535–736) were raised by Cocalico Biologicals in rabbits against GST-fusion proteins, which were expressed in *E. coli* and purified with glutathione beads. Affinity-purified antibodies were made from IgG, purified on a protein A Sepharose column, and eluted with 0.1 M glycine/HCl [pH 2.5] by binding to GST fusions to IP3R-1 or Rtn4a/NogoA, covalently coupled to Sepharose columns. The antibodies were eluted with 0.1 M glycine/HCl and cleared of GST antibodies on a GST Sepharose column. Antibodies to TRAPα and p97 were described previously (Dreier and Rapoport, 2000; Ye et al., 2004).

In Vitro Network Formation

A light membrane fraction from *Xenopus* egg extracts was prepared as previously described (Dreier and Rapoport, 2000). Membranes were washed twice in buffer A200 (50 mM HEPES-KOH [pH 7.5], 2.5 mM $MgCl_2$, 250 mM sucrose, 200 mM KCl). Network formation in 10 μl was performed by incubating washed membranes (~0.5 mg/ml final concentration) in buffer A200 containing 1 mM ATP and 0.5 mM GTP at 25ºC for 60 min unless otherwise indicated. For low-salt incubations, 200 mM KCl was replaced by 50 mM potassium acetate. Staining was performed with octadecyl rhodamine.

Aequorin-Based Ca^{2+} Efflux Assay

Aequorin luminescence assays were performed as described previously (Merz and Wickner, 2004), with modifications. Network formation reactions (34 μl) were incubated at 25ºC in 96-well plates in a Wallac luminometer in the presence of 0.5 mM GTP, 0.3 mM ATP, 8 μM coelenterazine, and 80 nM aequorin (Molecular Probes), and measurements were taken every 3 min. Calibration was done using buffered Ca^{2+} EGTA with Mg^{2+} standard solutions (Molecular Probes).

Modification with SH Reagents and Identification of Rtn4a/NogoA

All modification reactions were performed on washed membranes in buffer A200 by preincubation with SH reagents for 20 min at 25ºC prior to the addition of 1 mM DTT to stop the modification reaction. GTP and ATP were added to start the network formation reaction. To identify the maleimide biotin (MB) modified target, washed membranes (10 μg) were incubated for 20 min with 5 μM MB, treated with DTT, and solubilized in 1% Triton X-100. The extract was centrifuged and then incubated for 1 hr at 4ºC with 20 μl of monomeric avidin beads (Pierce). Bound proteins were eluted with 2 mM biotin, subjected to SDS-PAGE, and identified by mass spectrometry. To identify Rtn4a/NogoA modification sites, washed membranes (100 μg) were incubated with 10 μM N-ethylmaleimide (NEM) and pelleted to remove excess NEM. The membranes were solubilized in 1% NP40, and the extract was centrifuged to remove precipitates. Rtn4a/NogoA was immunoprecipitated with antibodies to its C terminus, followed by binding to protein A Sepharose. The immunoprecipitated material was reduced with 10 mM DTT and incubated with 25 mM iodoacetamide. Rtn4a/NogoA was then resolved by SDS-PAGE and analyzed by mass spectrometry. All mass spectrometry was performed by the Taplin BMS facility at Harvard Medical School.

Topology Experiments and Construction of DP1 and Rtn4c/NogoC Cysteine Mutants

All Rtn4c/NogoC and DP1 cysteine mutants were created from Rtn4c/NogoC-myc or HA-DP1 constructs by using the QuikChange Site-Directed Mutagenesis Kit (Stratagene). Maleimide PEG 5 kDa (MP) modification experiments were performed as previously described (Le Gall et al., 2004), with some changes. COS cells (4×10^5), transfected with DP1 or Rtn4c/NogoC constructs, were washed in HCN buffer (50 mM HEPES [pH 7.5], 150 mM NaCl, 2 mM $CaCl_2$) and then treated with 0.04% digitonin or 1% Triton X-100 for 20 min at 4ºC. Samples were incubated for 30 min at 4ºC with 1 mM MP in the absence or presence of 20 mM DTT. DTT and 1% Triton X-100 were then added to all samples. Following SDS-PAGE, immunoblotting was performed with anti-Myc, anti-HA, or anti-GRP94 (Santa Cruz).

Interaction between Yeast Rtn1p, Rtn2p, and Yop1p

Rtn1-TAP, Rtn2-TAP, or wild-type *MAT*α strains were transformed with Rtn1-HA or Rtn2-HA pYC2-URA (CEN) expression constructs, grown in SC-URA + 2% raffinose to OD ~ 2, and then grown for 24 hr in SC-URA + 2% raffinose + 2% galactose. Cells (0.1 g) were pelleted, washed, and resuspended in 1 ml wash buffer (50 mM HEPES [pH 7.5], 150 mM KCl, 1 mM EGTA, 1 mM EDTA, 5 mM $MgCl_2$, 5% glycerol) with 1% digitonin. Cells were broken in a bead beater, the sample was centrifuged, and the supernatant (250 μl) was then incubated with 100 μl 50% IgG Sepharose (Amersham) for 4 hr at 4ºC. The beads were pelleted, unbound material was collected, the beads were washed in buffer containing 0.5% digitonin, and bound proteins were eluted with SDS. Samples were analyzed by SDS-PAGE followed by immunoblotting with HA peroxidase at 1:1000.

Analysis of In Vivo CPY Trafficking

Pulse-chase experiments were performed as described previously, with minor differences (Heidtman et al., 2005). Wild-type and Δ*rtn1/rtn2/yop1* cells were grown at 30ºC to OD ~ 0.5 (40 ml). *Sec18-1* cells were grown at 23ºC and then transferred to 37ºC for 15 min. All cells were labeled with ^{35}S-Met promix (Amersham) for 7 min. Unlabeled methionine and cysteine were then added during the chase period, and cells were collected at different time points. Cell lysates were prepared by bead-beat lysis, and the labeled species were immunoprecipitated with CPY antibodies and analyzed by SDS-PAGE on a 4%–20% gradient gel.

Supplemental Data

Supplemental Data include nine figures and can be found with this article online at http://www.cell.com/cgi/content/full/124/3/573/DC1/.

ACKNOWLEDGMENTS

We thank A. Merz, B. DeDecker, R. Tomaino, C. Barlowe, and the Nikon imaging facility at HMS for help with experiments; A. Salic and S. Strittmatter for material; T. Mitchison for stimulating discussions; and B. Burton, A. Palazzo, M. Rolls, D. Finley, and D. Pellman for helpful comments. G.K.V. was supported by a Jane Coffin Childs Memorial Fund for Medical Research fellowship, W.A.P. was supported by the NIDDK intramural program, and J.M.R. was supported by The Rotary Foundation. T.A.R. is

supported by NIH grant GM052586 and is a Howard Hughes Medical Institute Investigator.

Received: September 26, 2005
Revised: October 31, 2005
Accepted: November 30, 2005
Published: February 9, 2006

REFERENCES

Baumann, O., and Walz, B. (2001). Endoplasmic reticulum of animal cells and its organization into structural and functional domains. Int. Rev. Cytol. *205*, 149–214.

Calero, M., Whittaker, G.R., and Collins, R.N. (2001). Yop1p, the yeast homolog of the polyposis locus protein 1, interacts with Yip1p and negatively regulates cell growth. J. Biol. Chem. *276*, 12100–12112.

Chen, M.S., Huber, A.B., van der Haar, M.E., Frank, M., Schnell, L., Spillmann, A.A., Christ, F., and Schwab, M.E. (2000). Nogo-A is a myelin-associated neurite outgrowth inhibitor and an antigen for monoclonal antibody IN-1. Nature *403*, 434–439.

Chou, T., Kim, K.S., and Oster, G. (2001). Statistical thermodynamics of membrane bending-mediated protein-protein attractions. Biophys. J. *80*, 1075–1087.

Dodd, D.A., Niederoest, B., Bloechlinger, S., Dupuis, L., Loeffler, J.P., and Schwab, M.E. (2005). Nogo-A, -B, and -C are found on the cell surface and interact together in many different cell types. J. Biol. Chem. *280*, 12494–12502.

Dreier, L., and Rapoport, T.A. (2000). In vitro formation of the endoplasmic reticulum occurs independently of microtubules by a controlled fusion reaction. J. Cell Biol. *148*, 883–898.

Du, Y., Ferro-Novick, S., and Novick, P. (2004). Dynamics and inheritance of the endoplasmic reticulum. J. Cell Sci. *117*, 2871–2878.

Farsad, K., and De Camilli, P. (2003). Mechanisms of membrane deformation. Curr. Opin. Cell Biol. *15*, 372–381.

Geng, J., Shin, M.E., Gilbert, P.M., Collins, R.N., and Burd, C.G. (2005). Saccharomyces cerevisiae Rab-GDI displacement factor ortholog Yip3p forms distinct complexes with the Ypt1 Rab GTPase and the reticulon Rtn1p. Eukaryot. Cell *4*, 1166–1174.

Ghaemmaghami, S., Huh, W.K., Bower, K., Howson, R.W., Belle, A., Dephoure, N., O'Shea, E.K., and Weissman, J.S. (2003). Global analysis of protein expression in yeast. Nature *425*, 737–741.

GrandPre, T., Nakamura, F., Vartanian, T., and Strittmatter, S.M. (2000). Identification of the Nogo inhibitor of axon regeneration as a Reticulon protein. Nature *403*, 439–444.

Heidtman, M., Chen, C.Z., Collins, R.N., and Barlowe, C. (2005). Yos1p is a novel subunit of the Yip1p-Yif1p complex and is required for transport between the endoplasmic reticulum and the Golgi complex. Mol. Biol. Cell *16*, 1673–1683.

Holmer, L., and Worman, H.J. (2001). Inner nuclear membrane proteins: functions and targeting. Cell. Mol. Life Sci. *58*, 1741–1747.

Iwahashi, J., and Hamada, N. (2003). Human reticulon 1-A and 1-B interact with a medium chain of the AP-2 adaptor complex. Cell. Mol. Biol. (Noisy-le-Grand) *49*, OL467–OL471.

Iwahashi, J., Kawasaki, I., Kohara, Y., Gengyo-Ando, K., Mitani, S., Ohshima, Y., Hamada, N., Hara, K., Kashiwagi, T., and Toyoda, T. (2002). Caenorhabditis elegans reticulon interacts with RME-1 during embryogenesis. Biochem. Biophys. Res. Commun. *293*, 698–704.

Joslyn, G., Carlson, M., Thliveris, A., Albertsen, H., Gelbert, L., Samowitz, W., Groden, J., Stevens, J., Spirio, L., Robertson, M., et al. (1991). Identification of deletion mutations and three new genes at the familial polyposis locus. Cell *66*, 601–613.

Klopfenstein, D.R., Klumperman, J., Lustig, A., Kammerer, R.A., Oorschot, V., and Hauri, H.P. (2001). Subdomain-specific localization of CLIMP-63 (p63) in the endoplasmic reticulum is mediated by its luminal alpha-helical segment. J. Cell Biol. *153*, 1287–1300.

Lee, M.C., Orci, L., Hamamoto, S., Futai, E., Ravazzola, M., and Schekman, R. (2005). Sar1p N-terminal helix initiates membrane curvature and completes the fission of a COPII vesicle. Cell *122*, 605–617.

Le Gall, S., Neuhof, A., and Rapoport, T. (2004). The endoplasmic reticulum membrane is permeable to small molecules. Mol. Biol. Cell *15*, 447–455.

Merz, A.J., and Wickner, W.T. (2004). Trans-SNARE interactions elicit Ca2+ efflux from the yeast vacuole lumen. J. Cell Biol. *164*, 195–206.

Oertle, T., and Schwab, M.E. (2003). Nogo and its paRTNers. Trends Cell Biol. *13*, 187–194.

Oertle, T., Klinger, M., Stuermer, C.A., and Schwab, M.E. (2003a). A reticular rhapsody: phylogenic evolution and nomenclature of the RTN/Nogo gene family. FASEB J. *17*, 1238–1247.

Oertle, T., van der Haar, M.E., Bandtlow, C.E., Robeva, A., Burfeind, P., Buss, A., Huber, A.B., Simonen, M., Schnell, L., Brosamle, C., et al. (2003b). Nogo-A inhibits neurite outgrowth and cell spreading with three discrete regions. J. Neurosci. *23*, 5393–5406.

Ostermeyer, A.G., Ramcharan, L.T., Zeng, Y., Lublin, D.M., and Brown, D.A. (2004). Role of the hydrophobic domain in targeting caveolin-1 to lipid droplets. J. Cell Biol. *164*, 69–78.

Parton, R.G., and Richards, A.A. (2003). Lipid rafts and caveolae as portals for endocytosis: new insights and common mechanisms. Traffic *4*, 724–738.

Prinz, W.A., Grzyb, L., Veenhuis, M., Kahana, J.A., Silver, P.A., and Rapoport, T.A. (2000). Mutants affecting the structure of the cortical endoplasmic reticulum in Saccharomyces cerevisiae. J. Cell Biol. *150*, 461–474.

Qi, B., Qi, Y., Watari, A., Yoshioka, N., Inoue, H., Minemoto, Y., Yamashita, K., Sasagawa, T., and Yutsudo, M. (2003). Pro-apoptotic ASY/Nogo-B protein associates with ASYIP. J. Cell. Physiol. *196*, 312–318.

Rolls, M.M., Stein, P.A., Taylor, S.S., Ha, E., McKeon, F., and Rapoport, T.A. (1999). A visual screen of a GFP-fusion library identifies a new type of nuclear envelope membrane protein. J. Cell Biol. *146*, 29–44.

Schweizer, A., Rohrer, J., Slot, J.W., Geuze, H.J., and Kornfeld, S. (1995). Reassessment of the subcellular localization of p63. J. Cell Sci. *108*, 2477–2485.

Sprong, H., van der Sluijs, P., and van Meer, G. (2001). How proteins move lipids and lipids move proteins. Nat. Rev. Mol. Cell Biol. *2*, 504–513.

Staehelin, L.A. (1997). The plant ER: a dynamic organelle composed of a large number of discrete functional domains. Plant J. *11*, 1151–1165.

Steiner, P., Kulangara, K., Sarria, J.C., Glauser, L., Regazzi, R., and Hirling, H. (2004). Reticulon 1-C/neuroendocrine-specific protein-C interacts with SNARE proteins. J. Neurochem. *89*, 569–580.

Tagami, S., Eguchi, Y., Kinoshita, M., Takeda, M., and Tsujimoto, Y. (2000). A novel protein, RTN-XS, interacts with both Bcl-XL and Bcl-2 on endoplasmic reticulum and reduces their anti-apoptotic activity. Oncogene *19*, 5736–5746.

Terasaki, M., Chen, L.B., and Fujiwara, K. (1986). Microtubules and the endoplasmic reticulum are highly interdependent structures. J. Cell Biol. *103*, 1557–1568.

van de Velde, H.J., Roebroek, A.J., Senden, N.H., Ramaekers, F.C., and Van de Ven, W.J. (1994). NSP-encoded reticulons, neuroendocrine proteins of a novel gene family associated with membranes of the endoplasmic reticulum. J. Cell Sci. *107*, 2403–2416.

Voeltz, G.K., Rolls, M.M., and Rapoport, T.A. (2002). Structural organization of the endoplasmic reticulum. EMBO Rep. *3*, 944–950.

Ye, Y., Shibata, Y., Yun, C., Ron, D., and Rapoport, T.A. (2004). A membrane protein complex mediates retro-translocation from the ER lumen into the cytosol. Nature *429*, 841–847.